

## STUDIES ON THE STATISTICAL ASEISMIC SAFETY OF RELATIVELY LONG PERIOD STRUCTURES

*Yoshikazu Yamada\**  
*Hirokazu Takemiya\*\**

### SYNOPSIS

The authors tried to study the aseismic safety, in a statistical sense, of relatively long period structures through dynamic analysis. The earthquake characteristics, the properties of structural dynamics and those of the foundation layer are the essential contributing factors to structural behaviours; therefore, they are included as parameters in the safety criterion deduced.

The statistical description of strong earthquakes is executed both for their random sequences of occurrence and for their individual random ground motions. Through the latter simulation, the nonstationary vibration of structures is investigated. The probability of failure by application of a finite duration of motion is obtained from the first-passage problem. By introduction of this quantity into the former assumed distribution function, the risk of failure of structures associated in their service period is evaluated.

The results are presented in an available spectrum form as the information on the aseismic integrity of a structural product.

### I. INTRODUCTION

Strong earthquakes which will destroy civil engineering structures are the rare events of stochastic nature. Such historical records available for detection of their properties count small, which makes indispensable their mathematical simulations. The structural dynamic analysis due to them is the most significant subject in aseismic engineering especially for long period structures.

The current codes and regulations of aseismic structural design provide no probabilistic measure of safety. Structures might as well be designed against earthquakes expected in future at their construction sites corresponding to their service-ability.

In this paper, earthquakes are composed of the two independent phenomena; one is a random ground motion with a finite duration and the other is its random sequences of occurrence with various intensities. As for the input form to structures, acceleration forms have been adopted by many researchers. But it should be determined according to the relation between input and structural system in frequency domain. Structures considered here having the relatively long period, the authors also assumed the input ground motions as accelerations. This assumption is, however, checked in their response analyses.

The response of a multi-degrees of freedom system is in general evaluated

---

\* Dr. Eng., Professor, Dept. of Civil Eng., Kyoto University

\*\* M.S., Assistant, Dept. of Transportation Eng., Kyoto University

by superposition of its individual mode shares. However, much attention should be paid to the system which has a multiple or closely proximated natural frequencies. In the system of their well separated, the R.M.S. value of each mode gives an adequate estimation of response, which was smaller than that in the former case<sup>1),2)</sup>. This means that the more rational design will be attained by finding the system with well separated natural frequencies. Hence, this paper is devoted to the investigation of a single degree of freedom system corresponds to its individual modes.

The safety of structures in random ground motion is at first treated from the standpoint of threshold crossing over the specified barrier. Next, the results are combined with the earthquake occurrence distribution function. The risk of failure of structures in their service period is thus deduced and the expected life time is evaluated as its inverse. The former is shown in a spectrum form for the specific locality.

## II. SEQUENCES OF EARTHQUAKE OCCURRENCES

A sequence of earthquake phenomena are the energy liberations at their foci when the accumulated one by inner lithosphere activities grows greater than the allowable strain energy of rock. Their theoretical description is very difficult due to many uncertainties involved. Thus, it is preferable to express those in a stochastic process model as that follows.

Herein, the occurrence of earthquakes is assumed to be governed by a Poisson Law.

$$P_n(t) = \frac{(ht)^n}{n!} e^{-ht} \quad (2.1)$$

where the parameter  $h$  is the reciprocal of the return period  $T_r$  and is found from the equation of

$$\sum_{l=1}^{\infty} n_l \frac{T_r}{T_e} = 1 \quad (2.2)$$

in which  $n_l$  is the numbers of earthquakes felt to be of intensity  $l$  in the entire recorded period  $T_e$ . This equation, however, is based on the time-invariant distribution function of occurrence over the whole period. A modification was made to the model for reasonable adequacy of the seismic activities in the period concerned; i.e., the earthquake occurrences have an identical distribution function only over the past interval  $T_p$  and the future  $T_f$ <sup>3)</sup>. Then, Eq. (2.2) is rewritten as

$$T_r = \frac{N_e T_p}{\sum_{l=1}^{\infty} n_l N_p} \quad (2.3)$$

where  $N_e$  is the total number of past recorded earthquakes, and  $N_p$  is that in  $T_p$ .

Concerning the seismic intensities, the historical records of more than 5 JMA scale are considered; for these have been closely related to structural failures. In Table 1 are listed their numbers at several localities, their calculated return

Table 1 Data of past earthquakes and calculated results

Locality	Number of past earthquakes				$T_p$	$N_p$	Probability of occurrence out of $N_e$ in $T_f$		Return period $T_r$		
	$n_V$	$n_{VI}$	$n_{VII}$	$N_e$			$T_f=75$ yrs	$T_f=100$ yrs	$n_V$	$n_{VI}$	$n_{VII}$
Kushiro	1	0	2	3	150	3	0.5000	0.6667	50	75	75
Sapporo	1	0	0	1	150	1	0.5000	0.6667	150	150	150
Akita	7	6	1	14	200	8	0.2143	0.2857	25	50	350
Sendai	9	1	1	11	200	7	0.2386	0.3182	29	157	314
Tokyo	14	10	7	31	200	15	0.1815	0.2419	13	24	59
Toyama	10	4	0	14	200	4	0.1071	0.1429	50	175	—
Nagoya	9	6	4	19	200	8	0.1579	0.2105	25	48	119
Kyoto	20	18	1	39	200	13	0.1250	0.1667	15	32	600
Hiroshima	5	3	1	9	200	4	0.1667	0.2222	50	113	450
Kochi	6	2	1	9	200	4	0.1667	0.2222	50	150	450
Fukuoka	2	0	0	2	200	1	0.1875	0.2500	200	—	—
Miyazaki	4	1	1	6	200	4	0.2500	0.3333	50	150	300

periods, and the probabilities of occurrence in the future interval of 75 and 100 years out of past total earthquakes.

### III. SIMULATION OF EARTHQUAKE MOTIONS

Strong ground motions, caused by earthquakes, have the nature of randomness affected by a large number of seismic integrants such as the dynamic properties of ground, the shock mechanism, the nature of geologic formation passed by seismic waves. It is essential for a structural design purpose to describe these non-repeatable and non-preestimative features in a mathematical expression. Their various forms have been proposed by many authors<sup>4),5),6),7),8)</sup>. V. V. Bolotin among them made a preferable one which belongs to a non-stationary stochastic process of<sup>9)</sup>

$$f(t) = \sum_p \phi_p(\alpha_1, \alpha_2, \dots, \alpha_r; t) g_p(\alpha_{r+1}, \alpha_{r+2}, \dots, \alpha_n; t) \quad (3.1)$$

This form means that the random process with time evolving can be expressed by the product of a stationary random process  $g(t)$  and a deterministic function  $\phi(t)$  which makes the former into a nonstationarity. The parameters involved represent the seismic integrants. Some ought to be subjected to a certain probability distribution and some are deterministic to a specified locality.

In this paper for approximation, the following is adopted.

$$f(t) = \phi(\alpha_1, \alpha_2; t) g(\alpha_3, \alpha_4, \alpha_5; t) \quad (3.2)$$

The deterministic function  $\phi(t)$  was built from the envelopes of actual strong accelerograms. The results give the form of

$$\phi(t) = (e^{-\alpha_1 t} - e^{-\alpha_2 t}) \cdot H(t) \quad (3.3)$$

where  $\alpha_1$  and  $\alpha_2$  are the positive constants through which the rapidity of rising up and decay of the seismic waves can be controlled.  $H(t)$  is the Heaviside unit

step function. Fig. 1 shows the deterministic function of 15 seconds duration, where the maximum point is located at  $(1/(\alpha_1 - \alpha_2) \cdot \log \alpha_1/\alpha_2, (\alpha_1/\alpha_2)^2)$ .

As the effects of local geophysical conditions on seismic waves are great, so the input power spectral density must be consistent with the characteristics of

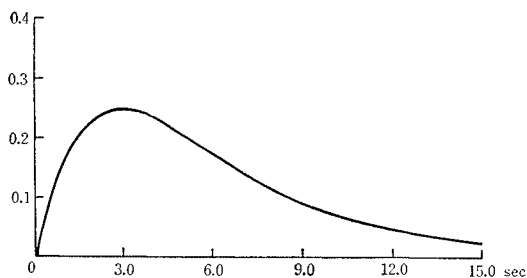


Fig. 1 Deterministic function  $\phi(t)$

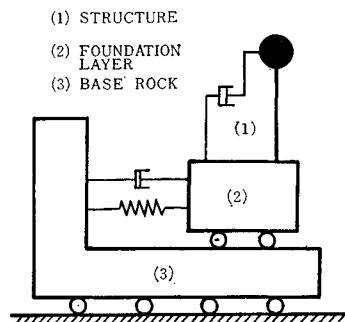


Fig. 2 Idealized system of foundation layer and structure

the foundation layer. Hence, the input stationary part  $g(t)$  is supposed as the absolute acceleration response passing a white noise through the foundation layer idealized with one degree of freedom system. The illustration is given in Fig. 2. Its governing equation of motion is

$$\ddot{X}_g(t) + 2\mu_g \dot{X}_g(t) + (\omega_g^2 + \mu_g^2)X_g(t) = n(t) \quad (3.4)$$

in which  $\omega_g$  and  $\mu_g$  represent the predominant frequency and the damping effects, respectively.  $n(t)$  is the white noise with mean zero and the correlation of

$$E\{n(t_1)n(t_2)\} = D \cdot \delta(t_2 - t_1) \quad (3.5)$$

where the constant  $D$  is its level of intensity. Then, from Eq. (3.4) the frequency response function of foundation layer is found for absolute acceleration as

$$H_g(i\omega) = \frac{2\mu_g(i\omega) + (\omega_g^2 + \mu_g^2)}{(i\omega)^2 + 2\mu_g(i\omega) + (\omega_g^2 + \mu_g^2)} \quad (3.6)$$

Its response power spectral density is obtained from the input-output relation in frequency domain of random variables.

$$S_g(\omega) = |H_g(i\omega)|^2 \cdot D = \frac{(\omega_g^2 + \mu_g^2)^2 + 4\mu_g^2\omega^2}{\{(\omega_g^2 + \mu_g^2) - \omega^2\}^2 + 4\mu_g^2\omega^2} \cdot D \quad (3.7)$$

The auto-correlation function is calculated by the inverse Fourier transformation of Eq. (3.7).

$$E\{g(t)g(t+\tau)\} = \frac{1}{2\pi} \int_{-\infty}^{\infty} S_g(\omega)e^{i\omega\tau} d\omega \quad (3.8)$$

The statistical properties of random variables  $f(t)$ , which mean the pseudo-earthquake motion, can only be evaluated in terms of their variance and covariance. By use of Eq. (3.2) and Eq. (3.8) substituted from Eq. (3.7), the latter is obtained such as

$$\begin{aligned}
 & E\{f(t_1)f(t_2)\} \\
 &= \frac{D}{4\mu_g\omega_g} \phi(t_1)\phi(t_2)e^{-\mu_g|t_2-t_1|} \{ \mu_g(\omega_g^2 - 3\mu_g^2) \sin \omega_g |t_2 - t_1| + \omega_g(\omega_g^2 + 5\mu_g^2) \cos \omega_g(t_2 - t_1) \}
 \end{aligned}
 \tag{3.9}$$

The variance is given by setting the time  $t_1=t_2=t$ .

The values of constants used for the simulation of ground motions are listed in Table 2. For their adequacy, comparison was made between stochastic characteristics of stationary process  $g(t)$  and those of actual strong acceleration records. Fig. 3 shows their normalized auto-correlation functions. Their power spectral densities are presented in Fig. 4. A slight difference is recognized between them; however, the intended use of this stochastic process presented is significant for the investigation of the general probabilistic response features of peak structures. In Fig. 5 is shown the time variation of standard deviation of input acceleration  $\sqrt{E\{f(t)^2\}}$ , where it is seen that the shape can also be modified to some extent by the parameters of  $\omega_g$  and  $\mu_g$ . Fig. 6 is an example of the stationary stochastic waves, generated by the computer from the power spectral density of Eq. (3.7)<sup>10</sup>. The recorded accelerogram of EL CENTRO, NS component is presented in Fig. 7 for comparison.

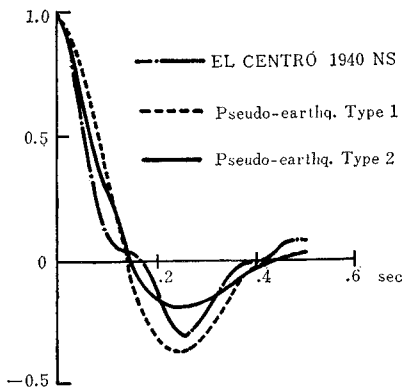


Fig. 3 Auto-correlation function of  $g(t)$

Table 2 Values of constants used for the simulation of earthquake motion

Pseudo-earthq. motion	Values of parameters			
	$\alpha_1$	$\alpha_2$	$\omega_g$	$\mu_g$
Type 1	0.25	0.50	12.3	3.86
Type 2	0.25	0.50	10.88	6.28

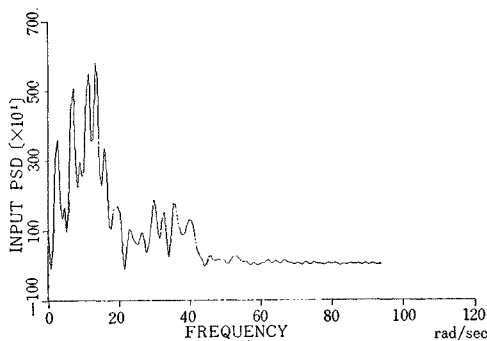


Fig. 4(a) Power spectral density of EL CENTRO earthquake 1940, NS component

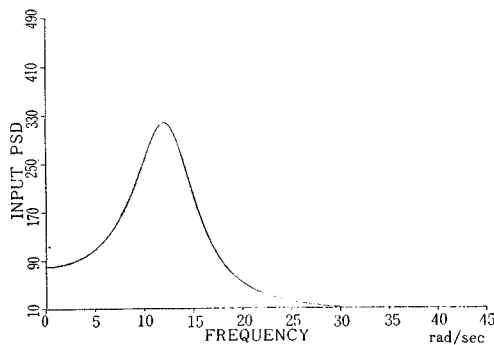


Fig. 4(b) Power spectral density assumed for pseudo-earthquake motion

Fig. 5 Standard deviation of input acceleration

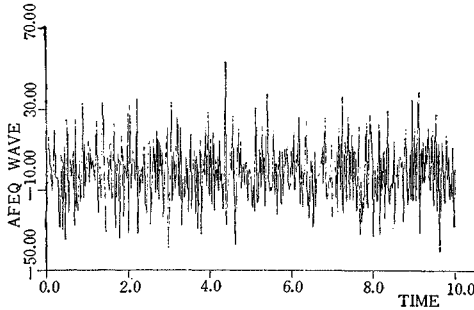
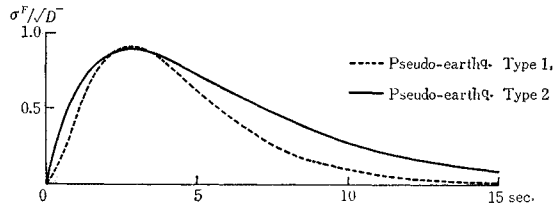


Fig. 6 Artificial earthquake generated

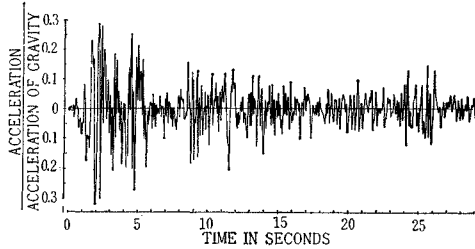


Fig. 7 EL CENTRO earthquake 1940, NS component

#### IV. RESPONSE ANALYSIS OF STRUCTURES

In the response analysis of structures, it is expedient to use the normal mode co-ordinates corresponding to their degrees of freedom. Then, the effects of each mode are superposed into a structural response.

Let  $y(x, t)$ ,  $X_i(x)$  and  $q_i(t)$  be the structural displacement response, the modal shape function, and the time function of  $i$ -th mode, respectively. By putting

$$y(x, t) = \sum_{i=1}^N X_i(x) q_i(t) \quad (4.1)$$

where  $N$  is the number of degrees of freedom, substitution of this expression is made into the governing equation of motion of

$$[M]\{\ddot{y}\} + [C]\{\dot{y}\} + [K]\{y\} = \{\bar{f}\} \quad (4.2)$$

in which the notations  $[M]$ ,  $[C]$ ,  $[K]$ , and  $\{\bar{f}\}$  represent the mass matrix, the damping matrix, the stiffness matrix of the system, and the external force, respectively. As the results, a sequence of independent equations are obtained provided that the damping term is a specific form of being separated in the modal co-ordinates<sup>(1), (2), (11)</sup>.

$$q(t) + 2\zeta\omega_0\dot{q}(t) + \omega_0^2q(t) = -f(t) \quad (4.3)$$

The multi-degrees of freedom systems, therefore, can be treated as one degree of freedom of individual modes, where the notations  $q_i$ ,  $\omega_{i0}$ ,  $\zeta_i$ , and  $f_i$  are replaced by  $q$ ,  $\omega$ ,  $\zeta$  and  $f$ .

The response of the system of Eq. (4.3) is given in terms of an impulsive response function  $h(t)$  in a form of convolution integral.

$$q(t) = - \int_0^t h(t-\tau) f(\tau) d\tau \quad (4.4)$$

where

$$h(t) = \frac{1}{\omega_a} \cdot e^{-\zeta\omega_0 t} \sin \omega_a t, \quad \omega_a = \omega_0 \sqrt{1 - \zeta^2} \quad (4.5)$$

The velocity response is the time derivative of Eq. (4.4).

$$\dot{q}(t) = - \int_0^t \dot{h}(t-\tau) f(\tau) d\tau \quad (4.6)$$

where

$$\dot{h}(t) = \frac{1}{\omega_a} \cdot e^{-\zeta\omega_0 t} (\omega_a \cos \omega_a t - \zeta\omega_0 \sin \omega_a t) \quad (4.7)$$

Excitations in Eq. (4.4) or Eq. (4.6) being defined only in a statistical sense, the responses are to be given by the stochastic characteristics such as the variance of displacement, velocity and acceleration, and their covariances. They are formularized in one expression as

$$\sigma^2(t:l, m) = \int_0^t \int_0^t \frac{\partial^l}{\partial t^l} h(t-\tau_1) \frac{\partial^m}{\partial t^m} h(t-\tau_2) \cdot E\{f(\tau_1) f(\tau_2)\} d\tau_1 d\tau_2 \quad (4.8)$$

where  $l$  and  $m$  take the integer of zero through 2. Substitution of Eq. (4.8) from Eq. (3.9) of excitation and Eq. (4.5) or Eq. (4.7) of impulsive response function gives the variance of displacement of

$$\sigma^2(t:0, 0) = \frac{D \cdot e^{-2\zeta\omega_0 t}}{4\mu_\sigma \omega_\sigma \omega_a^2} \sum_{i=1}^2 \sum_{j=1}^2 \{C1(i, j)I(i, j) + C2(i, j)J(i, j)\} \quad (4.9)$$

the covariance between displacement and velocity of

$$\begin{aligned} \sigma^2(t:0, 1) = & \frac{D \cdot e^{-2\zeta\omega_0 t}}{4\mu_\sigma \omega_\sigma \omega_a^2} \left[ \omega_a \sum_{i=1}^2 \sum_{j=1}^2 \{C1(i, j)K(i, j) + C2(i, j)L(i, j)\} \right. \\ & \left. - \zeta\omega_0 \sum_{i=1}^2 \sum_{j=1}^2 \{C1(i, j)I(i, j) + C2(i, j)J(i, j)\} \right] \quad (4.10) \end{aligned}$$

and the variance of velocity of

$$\begin{aligned} \sigma^2(t:1, 1) = & \frac{D \cdot e^{-2\zeta\omega_0 t}}{4\mu_\sigma \omega_\sigma \omega_a^2} \left[ \omega_a^2 \sum_{i=1}^2 \sum_{j=1}^2 \{C1(i, j)M(i, j) + C2(i, j)N(i, j)\} \right. \\ & - 2\zeta\omega_0 \omega_a \sum_{i=1}^2 \sum_{j=1}^2 \{C1(i, j)K(i, j) + C2(i, j)L(i, j)\} \\ & \left. + (\zeta\omega_0)^2 \sum_{i=1}^2 \sum_{j=1}^2 \{C1(i, j)I(i, j) + C2(i, j)J(i, j)\} \right] \quad (4.11) \end{aligned}$$

where

$$C1(1, 1) = -C1(1, 2) = -C1(2, 1) = C1(2, 2) = \mu_\sigma (\omega_\sigma^2 - 3\mu_\sigma^2)$$

$$C2(1, 1) = -C2(1, 2) = -C2(2, 1) = C2(2, 2) = \omega_\sigma (\omega_\sigma^2 + 5\mu_\sigma^2)$$

$$\begin{aligned}
I(i, j) &= \int_0^t \int_0^t e^{\xi(\tau_1, \tau_2)} SS(t; \tau_1, \tau_2) \sin \omega_g |\tau_1 - \tau_2| d\tau_1 d\tau_2 \\
J(i, j) &= \int_0^t \int_0^t e^{\xi(\tau_1, \tau_2)} SS(t; \tau_1, \tau_2) \cos \omega_g (\tau_1 - \tau_2) d\tau_1 d\tau_2 \\
K(i, j) &= \int_0^t \int_0^t e^{\xi(\tau_1, \tau_2)} SC(t; \tau_1, \tau_2) \sin \omega_g |\tau_1 - \tau_2| d\tau_1 d\tau_2 \\
L(i, j) &= \int_0^t \int_0^t e^{\xi(\tau_1, \tau_2)} SC(t; \tau_1, \tau_2) \cos \omega_g (\tau_1 - \tau_2) d\tau_1 d\tau_2 \\
M(i, j) &= \int_0^t \int_0^t e^{\xi(\tau_1, \tau_2)} CC(t; \tau_1, \tau_2) \sin \omega_g |\tau_1 - \tau_2| d\tau_1 d\tau_2 \\
N(i, j) &= \int_0^t \int_0^t e^{\xi(\tau_1, \tau_2)} CC(t; \tau_1, \tau_2) \cos \omega_g (\tau_1 - \tau_2) d\tau_1 d\tau_2 \\
SS(t; \tau_1, \tau_2) &= \sin \omega_d (t - \tau_1) \sin \omega_d (t - \tau_2) \\
SC(t; \tau_1, \tau_2) &= \sin \omega_d (t - \tau_1) \cos \omega_d (t - \tau_2) \\
CC(t; \tau_1, \tau_2) &= \cos \omega_d (t - \tau_1) \cos \omega_d (t - \tau_2) \\
\xi(\tau_1, \tau_2) &= \beta_i \tau_1 + \beta_j \tau_2 - \mu_g |\tau_1 - \tau_2| \\
\beta_i &= \zeta \omega_0 - \alpha_i
\end{aligned}$$

The double integral on  $t$  was evaluated after some tedious algebraic operations.

On the other hand, from stationary response analysis, the stationary asymptotes are found for the displacement and velocity as

$$\sigma^2(\infty; 0, 0) = \frac{S_g(\omega_0)}{4\zeta\omega_0^3} \quad (4.12)$$

$$\sigma^2(\infty; 1, 1) = \frac{S_g(\omega_0)}{4\zeta\omega_0} \quad (4.13)$$

However, the one for displacement, deduced by T. K. Caughey, is multiplied by the constant  $\pi^{12}$ . This is due to the relation between the auto-correlation and the power spectral density, linked by the Fourier transform. Here, the transformation of Eq. (3.8) and its pair are utilized. The effect of nonstationarity on seismic intensity is, moreover, taken into account multiplying Eq. (4.12) by  $(\alpha_1/\alpha_2)^4$ . The response barrier for the latter analysis is then determined as the  $\gamma$  times of

$$\sigma^*(\infty; 0, 0) = \sqrt{\frac{\pi S_g(\omega_0)}{4\zeta\omega_0^3}} \left( \frac{\alpha_1}{\alpha_2} \right)^2 \quad (4.14)$$

Figs. 8, 9 and Fig. 10 show the time variations of above response characteristics. The stationary asymptotes are also presented there, comparing the effects of nonstationarity of excitations on responses. From Fig. 8 and Fig. 9, it is understood that the system continues to vibrate after the termination of input, especially so in the longer period one. Figs. 10(a) and (b) show that the covariance tends to approach to a constant value after the time a few times of natural



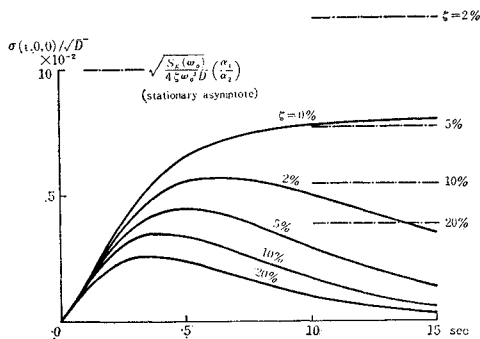


**Fig. 8** Standard deviation of displacement response, pseudo-earthq. Type 2 natural freq.  $\omega_0=4.0$  rad/sec

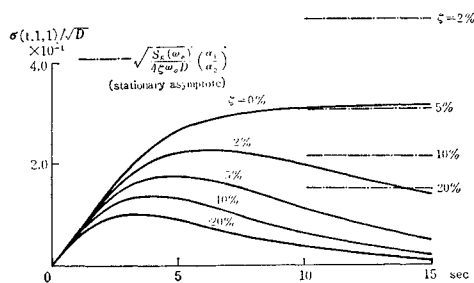


**Fig. 9** Standard deviation of velocity response, pseudo-earthq. Type 2 natural freq.  $\omega_0=4.0$  rad/sec

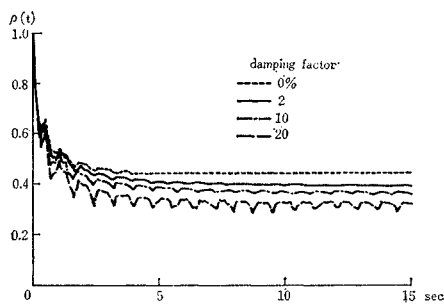


**Fig. 10(a)** Correlation function  $\rho(t)$  of displacement and velocity, pseudo-earthq. Type 2 natural freq.  $\omega_0=4.0$  rad/sec

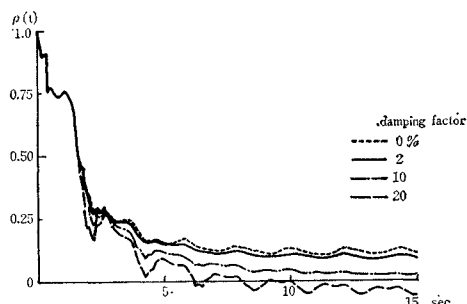


**Fig. 10(b)** Correlation function  $\rho(t)$  of displacement and velocity, pseudo-earthq. Type 2 natural freq.  $\omega_0=1.2$  rad/sec

period, with the periodicity of its one half in the heavily damped systems. The asymptote reduces inversely as the increase of natural period and this tendency is forwarded by the damping effect. These results explain that the correlation between displacement and velocity disappears in the peak structure of natural period longer than about 6 seconds per cycle and the former dominates the system response. Such a phenomenon may suggest that structures longer than that period prefer displacements to accelerations as the input form of excitations.

The adequacy of the input form as acceleration is checked by the response spectra from actual strong earthquake records. Figs. 11, 12 and Fig. 13 are the stochastic response spectra obtained from the maximum standard deviations of displacement, velocity, and acceleration, respectively. These figures make a good coincidence with the results by Housner<sup>13)</sup>.

Simplifications were made for the above spectra such as in Fig. 14. Their inspections indicate that structures are grouped from the view point of dynamic design; one is the longer period than  $T_0$  and the other the shorter than it. The value of  $T_0$  was chosen as 0.5 sec/c. The former shows a constant velocity spectrum and an increase displacement one proportional to natural period. The

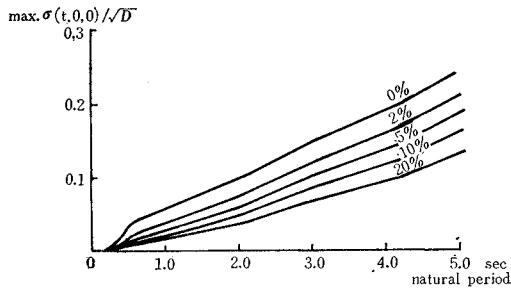


Fig. 11 Deformation spectra

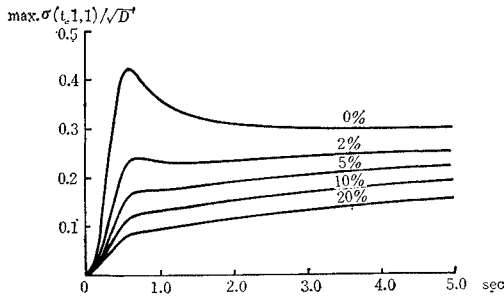
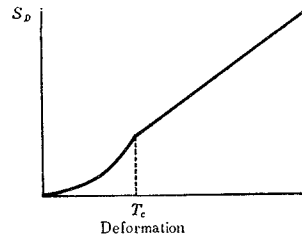


Fig. 12 Velocity spectra

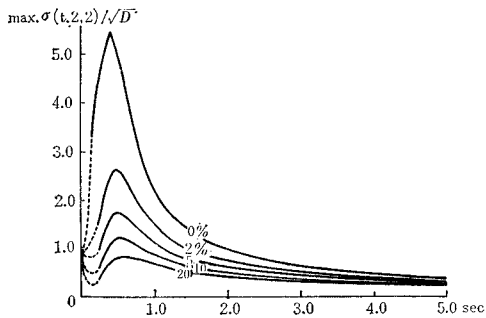
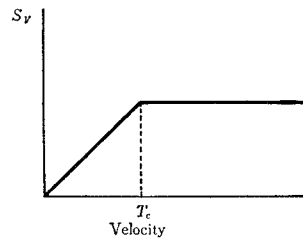


Fig. 13 Acceleration spectra

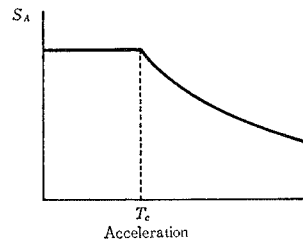


Fig. 14 Idealized response spectra

dynamic safety, therefore, can be evaluated from the threshold crossing theory over the displacement barrier specified. The latter has a constant acceleration spectrum and an increase velocity one proportional to natural period. In this case only the consideration of dominant acceleration is enough for structural design.

### V. SAFETY EVALUATION OF STRUCTURES

In this chapter is dealt in the basic concept of safety and reliability of structures against earthquakes in their service period. Failure is herein defined as the response first-exursion over the specified barrier.

If the response is assumed to be a random process subjected to the two

dimensional Gaussian distribution function of displacement  $y$  and velocity  $\dot{y}$ , its probability density is defined by

$$p(y, \dot{y}; t) = \frac{1}{2\pi\sigma(t:0,0)\sigma(t:1,1)\sqrt{1-\rho^2}} \exp \left[ -\frac{1}{2(1-\rho^2)} \left\{ \left( \frac{y}{\sigma(t:0,0)} \right)^2 - \frac{2\rho}{\sigma(t:0,0)\sigma(t:1,1)} y \dot{y} + \left( \frac{\dot{y}}{\sigma(t:1,1)} \right)^2 \right\} \right] \quad (5.1)$$

where

$$\rho(t) = \frac{\sigma^2(t:0,1)}{\sigma(t:0,0)\sigma(t:1,1)} \quad (5.2)$$

The expected number with upward crossing over the barrier  $B$  per unit time is given by S. O. Rice as<sup>14)</sup>

$$E[N_+(B, t)] = \int_0^\infty \dot{y} p(B, \dot{y}; t) d\dot{y} \quad (5.3)$$

Substitution of Fq. (5.1) into Eq. (5.3) yields

$$E[N_+(B, t)] = \frac{1}{2\pi} \cdot \frac{\sigma(t:1,1)}{\sigma(t:0,0)} \exp \left\{ -\frac{1}{2} \left( \frac{B}{\sigma(t:0,0)} \right)^2 \right\} \times \left[ \sqrt{1-\rho^2} \exp \left\{ -\frac{\rho^2}{2(1-\rho^2)} \left( \frac{B}{\sigma(t:0,0)} \right)^2 \right\} + \frac{\pi}{2} \rho \left( \frac{B}{\sigma(t:0,0)} \right) \left\{ 1 + \operatorname{erf} \left( \frac{\rho}{\sqrt{2(1-\rho^2)}} \frac{B}{\sigma(t:0,0)} \right) \right\} \right] \quad (5.4)$$

The initial conditions of displacement and velocity being zero make the result of

$$E[N(|B|, t)] = 2E[N_+(B, t)] \quad (5.5)$$

Then, as the upper bound of the probability of crossing, the expected total number for every set of excitations is obtained by integration over the earthquake duration  $t_r$ .

$$N_{\text{total}} = 2 \int_0^{t_r} E[N_+(B, t)] dt \quad (5.6)$$

For the relatively small barrier  $B$  and the large value of  $t_r$ , however, there remains the fault in Eq. (5.6); that is, the effect of previous crossings over the barrier on successive ones is not taken into account. The renewal process may be effectively utilized in this case. But in this study from the definition of failure, the barrier to be specified is so high that the probability of crossing over it becomes statistically rare. The concept of first-occurrence time density can thus well be applied in its limiting case<sup>15)</sup>. It is deduced as

$$P_{f.o.t.}(B, t) = E[N_+(B, t)] \exp \left\{ -\int_0^t E[N_+(B, \tau)] d\tau \right\} \quad (5.7)$$

The probability of failure by one earthquake is obtained by integration of Eq. (5.7) over its duration.

$$P_f(|B|, t_T) = \int_0^{t_T} P_{f.o.t.}(|B|, t) dt \tag{5.8}$$

Substituting Eq. (5.7) into Eq. (5.8), with consideration of Eq. (5.5), yields

$$P_f(|B|, t_T) = 2 \left[ 1 - \exp \left\{ - \int_0^{t_T} E[N_+(B, t)] dt \right\} \right] \tag{5.9}$$

Fig. 15 shows the number of threshold crossing per unit time over the barrier  $B$  which was chosen such as

$$B = \gamma \cdot \sigma^*(\infty; 0, 0) \tag{5.10}$$

The multiplier  $\gamma$  to the specific value  $\sigma^*(\infty; 0, 0)$  is taken as 1/3, 2/3, 1.0, 4/3, 5/3, 2.0. Fig. 16 gives the spectrum of probability of failure  $P_f$  by one pseudo-earthquake motion, Type 2 simulated in Chap. 3. In view of this figure, it is recognized that the frequency characteristics of ground motion as well as its non-stationarity affect significantly the probability of failure  $P_f$ . It decreases gradually in proportion to the natural period of structures in the range larger than 1.0 sec/c. A notch appears, due to the parameters characterizing the foundation

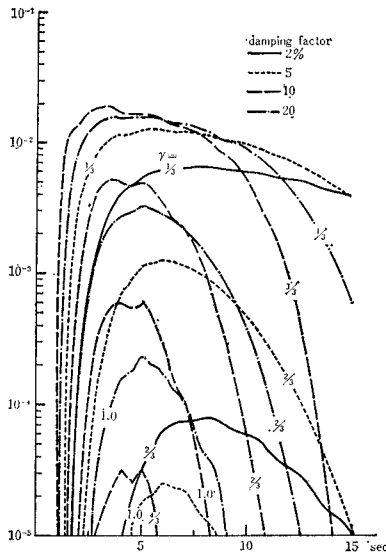


**Fig. 15** Number of threshold crossing per unit time, pseudo-earthq. Type 2  
natural freq.  $\omega_0 = 4.0$  rad/sec

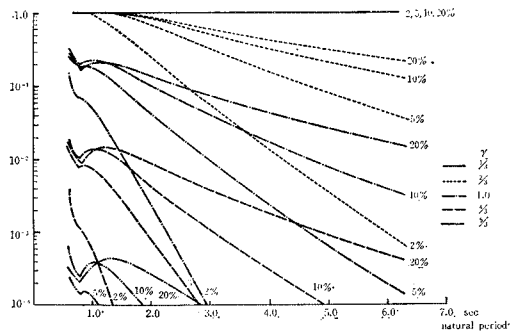


**Fig. 16** Probability of failure by one earthquake motion, pseudo-earthq. Type 2

layer, at its predominant period. In the period range shorter than that, the probability of failure is strongly inversely as the natural period. But this phenomenon is caused by the fact that the dominant response comes out as velocity or acceleration rather than displacement. The structural damping affects the evaluation of  $P_f$  a little in the shorter period range and greatly in the longer. But the probabilities  $P_f$  are roughly grouped by the value of  $\gamma$ .

The quantity  $P_f$  obtained above is not a life-range measure of safety of structures subjected to random sequences of earthquake occurrence. The probability of structural survival, taken from their distribution function  $P_n(t)$ , is very significant. Such a probability function is defined as a reliability function by A. M. Freudenthal<sup>16)</sup>, and expressed as

$$L_{T_i}(T_i^*) = P_r(T_i > T_i^*) \tag{5.11}$$

where the structural life  $T_i$  is a random variable and  $T_i^*$  is a certain specified life time.

Let the seismic loadings which induce the structural failure  $P_f$  in each duration be subjected to the distribution  $F_s(y)$  in their occurrence history and the structural resistance to their applications be to the distribution function  $F_r(y)$ . Then, the reliability function of Eq. (5.11) against failure is formulated as

$$L_{T_i}(t) = \int_0^\infty \sum_{k=0}^\infty \frac{(ht)^k}{k!} \cdot e^{-ht} [F_s(y)]^k f_r(y) dy \tag{5.12}$$

where  $f_r(y)$  is the probability density of  $F_r(y)$ .

As has been mentioned in Chap. 1, the seismic risk of structures is estimated by their dynamic analysis, depending upon the earthquake simulation both for its random sequences of occurrence and for its random ground motions. The former was assumed to be a Poisson process in Chap. 2, where seismic intensities are taken into account in terms of their return period. The mathematical expression for the latter was made independently of seismic intensity. On the other hand, let the structural resistance remain also unchanged after sequences

of earthquake until the complete failure. This method of analysis makes the probabilities of structural failure due to them into constant values. Then, Eq. (5.12) can be simplified as

$$L_{T_i}(t) = \sum_{k=0}^\infty \frac{(ht)^k}{k!} \cdot e^{-ht} (1 - P_f)^k \doteq e^{-hP_f t} \tag{5.13}$$

The probability of failure during the structural life is found as

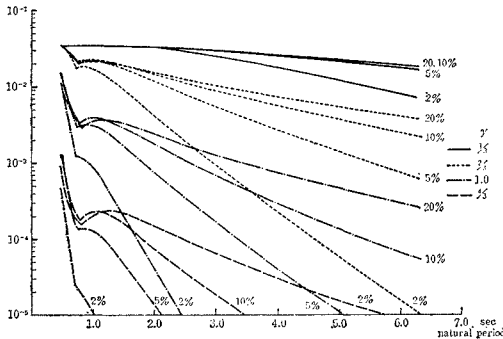


**Fig. 17 Risk of failure**  
Pseudo-earthq. Type 2,  $1/T_r = 0.0169$

$$F_{T_i}(t) = 1 - L_{T_i}(t) \tag{5.14}$$

The longevity distribution  $f_{T_i}(t)$  and the risk of failure  $R_{T_i}(t)$  are thus

$$f_{T_i}(t) = \frac{dF_{T_i}(t)}{dt} = -\frac{dL_{T_i}(t)}{dt} \doteq hP_f e^{-hP_f t} \tag{5.15}$$

$$R_{T_i}(t) = \frac{f_{T_i}(t)}{L_{T_i}(t)} = -\frac{dL_{T_i}(t)}{L_{T_i}(t) dt} \doteq hP_f \tag{5.16}$$

In Figs. 17, 18 and Fig. 19, as examples of extensive numerical calculation, are shown the spectrum of risk of structural failure, the probability of structural failure

during the life, and the longevity distribution function, respectively. Figs. 20(a) and (b) are the spectra of probability of failure after 100 years, obtained from earthquake records more than 5 JMA scale and 7 JMA scale at Tokyo district. From these figures it is evidently understood that the input characteristics as well as structural dynamic properties are significant on the evaluation of structural safety. The risk of failure, as is evident from Eq. (5.16), is proportional to the probability of failure by one earthquake, and its proportional constant is the reciprocal of return period of earthquakes concerned. The longevity distribution

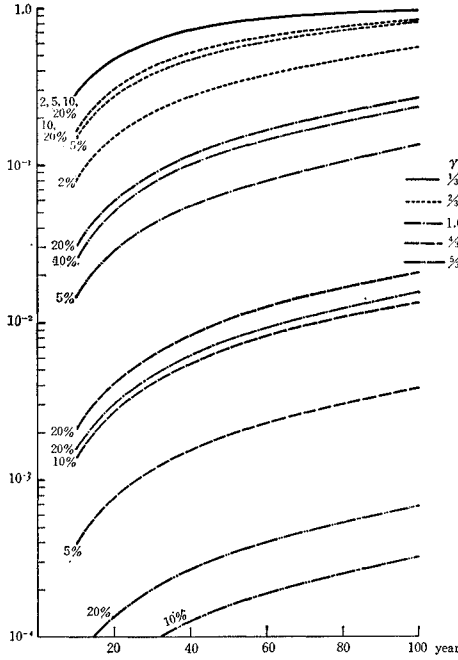


**Fig. 18** Failure probability  
Pseudo-earthq. Type 2,  $1/T_r=0.0169$ ,  
 $\omega_0=4.0$  rad/sec

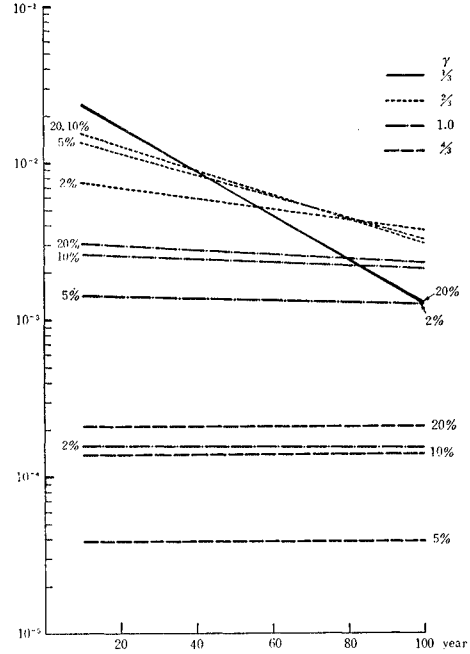


**Fig. 19** Longevity distribution  
Pseudo-earthq. Type 2,  $1/T_r=0.0169$ ,  
 $\omega_0=4.0$  rad/sec

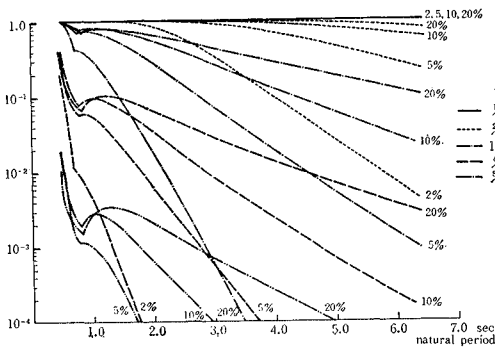


**Fig. 20(a)** Probability of failure after 100 years  
Pseudo-earthq. Type 2,  $1/T_r=0.0769$

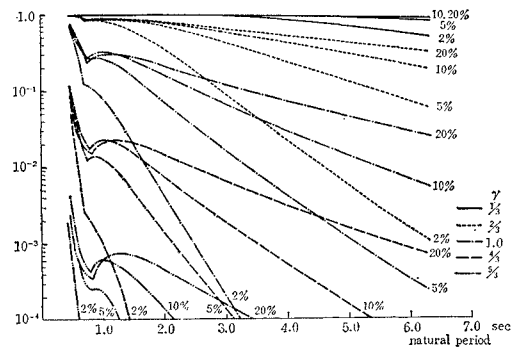


**Fig. 20(b)** Probability of failure after 100 years  
Pseudo-earthq. Type 2,  $1/T_r=0.0169$

shows the straight lines on logarithmic graph, where the correspondings to  $\gamma=1/3$  have a steep tangent while the ones to  $\gamma$  more than 1.0 are gentle or horizontal. The damping effect works for declivity. This tangent represents the acceleration of structural failure. In view of the aseismic design, the horizontal or the gentle slope is preferable. From Fig. 20, the influence of the return period  $T_r$  on the structural failure is within the order estimation while that of the multiplier  $\gamma$  is great. This suggests that the criterion concerning the response barrier can be determined for the specific locality; e.g. for peak structures at Tokyo district, the value of  $\gamma=1.0$  is proper in the range of about 1~4 sec/c period and  $\gamma=2/3$  in 4~6 sec/c. The increase of damping effect, however, gives an estimation of dangerous side.

## VI. CONCLUSIONS

The following conclusions may be derived from the results of this analytical study.

- 1) The input form of ground motions is evidently accelerations to the structures of natural period less than about 6 seconds per cycle while those to structures more than that period may be regarded as displacements.
- 2) The pseudo-earthquake motions simulated as acceleration are the reasonable ones, including both the stochastic parameters and the deterministic to the locality specified.
- 3) The rational aseismic design of relatively long period structures is effectively made on the response analysis. In this case the nonstationarity of input and the dynamic properties of structures are significant for their behaviours.
- 4) The seismic risk or the safety of structures against earthquakes in their service period is one of the most important integrants for aseismic design. The response barrier criterion deduced in respect to that is as follows:

$$B = \gamma \sqrt{\frac{\pi S_g(\omega_0)}{4\zeta\omega_0^3}} \left(\frac{\alpha_1}{\alpha_2}\right)^2$$

e.g. for specific locality, Tokyo, the value of  $\gamma$  is

- $\gamma=1.0$ : for structures of natural period between 1~4 sec/c  
 $\gamma=2/3$ : for structures of natural period between 4~6 sec/c

The more well-advised criterion may be determined as a function of an appropriate probability of failure, including the strength of materials and the serviceability of structure itself.

## BIBLIOGRAPHY

- 1) Y. Yamada and H. Takemiya: Studies on the Response of Multi-degrees of Freedom Systems Subjected to Random Excitation with Applications to the Tower and Pier Systems of Long Span Suspension Bridges, Memoirs of Faculty of Engineering, Kyoto Univ., Vol. 30, Part 4, 1968, pp. 371-396.
- 2) Y. Yamada and H. Takemiya: Studies on the Response of Multi-degrees of Freedom Systems Subjected to Random Excitation with Applications to the Tower and Pier Systems of Long Span Suspension Bridges, Trans. JSCE, No. 163, March 1969, pp. 17-27.

- 3) H. Goto and H. Kameda: A Statistical Study of the Maximum Ground Motion in Strong Earthquakes, Trans. JSCE, No. 159, Nov. 1968, pp. 1-12.
- 4) J. L. Bogdanoff, J. E. Goldberg and M. Bernard: Response of a Simple Structure to a Random Earthquake-Type Disturbance, Bull. Seismol. Soc. Amer., Vol. 51, No. 2, April 1961, pp. 293-310.
- 5) Y. K. Lin: Nonstationary Excitation and Response in Linear Systems Treated as Sequences of Random Pulses, J. Acoust. Soc. Am., 38, pp. 453-460 (1965).
- 6) M. Shinozuka and Y. Sato: Simulation of Nonstationary Process, Journal of the Engineering Mechanics Division, ASCE, Vol. 93, No. EM1, 1967, pp. 11-40.
- 7) Mohammad Amin and Alfredo H.-S. Ang.: Nonstationary Stochastic Model of Earthquake Motion, Proc. ASCE, Vol. 94, No. EM2, April 1968, pp. 559-583.
- 8) H. Goto and K. Toki: Structural Response to Nonstationary Random Excitation, Proc. of the 4th WCEE, Santiago, 1969, pp. 130-144.
- 9) V. V. Bolotin: Statistical Methods in Structural Mechanics, Second Revised and Augmented Edition, STRDIIZDAT, Moscow, 1965, Chap. 7.
- 10) H. Goto, K. Toki and T. Akiyoshi: Generation of Artificial Earthquakes on Digital Computer for Aseismic Design of Structures, Proc. of Japan Earthquake Engineering Symposium, Oct. 1966, pp. 25-30.
- 11) Walter C. Hurty and Moshe F. Rubinstein: Dynamics of Structures, Prentice-Hall, 1964, Chap. 8.
- 12) T. K. Caughey and H. J. Stumpf: Transient Response of a Dynamic System under Random Excitation, J. Appl. Mech., 28, pp. 563-566 (1961).
- 13) Housner: Vibration of Structures Induced by Seismic Waves, Shock and Vibration Handbook by Harris, C. M. Crede, C. E., pp. 522, 12-14.
- 14) S. O. Rice: Mathematical Analysis of Random Noise, Selected Papers on Noise and Stochastic Process, Dover, 1954, pp. 133-294.
- 15) J. R. Rice and F. P. Beer: First-Occurrence Time of High-level Crossings in a Continuous Random Process, J. Acoust. Soc. Am., April 1965, pp. 323-335.
- 16) A. M. Freudenthal, J. M. Garrelts and M. Shinozuka: The Analysis of Structural Safety, Journal of the Structural Division, ASCE, Vol. 92, No. ST1, 1966, pp. 267-325.

*(Received May 12, 1969)*